Crystal Structure and Magnetic Properties of $K_{5.5}Na_{1.5}[PW_{10}Cu_2(H_2O)_2O_{38}]\cdot 13H_2O$. Substituted Keggin Heteropolytungstates of the Type $PW_{10}Cu_2$ Containing Exchange-Coupled Copper Pairs

C. J. Gómez-Garcia,† E. Coronado,*,† P. Gómez-Romero,‡ and N. Casañ-Pastor‡

Departamento de Quimica Inorgánica, Universidad de Valencia, 46100 Burjassot, Valencia, Spain, and Institut de Ciencia de Materials de Barcelona, CSIC, Campus UAB, 08193 Bellaterra, Barcelona, Spain

Received February 24, 1992

We report the structural and magnetic characterization of the crystalline product obtained from a solution containing Δ-$(PW_9O_{34})^{9-}$ and Cu^{2+} ions (molar ratio 1/2) after standing a long period of time at room temperature. Three complementary techniques were used: X-ray diffraction, magnetic susceptibility measurements, and EPR spectroscopy. The crystals (space group $Fm3m$, a = 21.329 (4) Å, Z = 8) consist primarily of the potassium–sodium salt of the two cocrystallized heteropoly complexes, each formulated $[PW_{10}Cu_2(H_2O)_2O_{38}]^{7-}$, in both of which two Cu^{2+} ions have replaced the two W atoms of the well-known 12-tungsten α-Keggin structure. The compound can be formulated as $K_{5.5}Na_{1.5}[PW_{10}Cu_2(H_2O)_2O_{38}]\cdot 13H_2O$. Although in the crystals the sites of the two Cu atoms are disordered over the 12 possible locations in each anion's structure, magnetic techniques (susceptibility measurements and EPR spectroscopy) show that in each disubstituted Keggin complex, the two copper ions are preferentially occupying neighboring sites, giving rise to two isomers wherein the CuO_6 octahedra share a corner or an edge. These exchange-coupled pairs are characterized by two different exchange interactions and two different anisotropies. The best fit of the magnetic data indicates that only a small proportion of Keggin units contain nonadjacent Cu's (~8.5%).

Introduction

Heteropolyoxometalates have been shown to provide ideal structural supports for the study of magnetic interactions between paramagnetic metals,[1] as well as between delocalized "blue" electrons and paramagnetic metals.[2] Interested by the magnetic properties of this class of compounds, we have focused[3] on the series $[M_4(H_2O)_2(PW_9O_{34})_2]^{10-}$ and $[M_4(H_2O)_2(P_2W_{15}O_{56})_2]^{16-}$ (M = Co^{2+}, Cu^{2+}, Zn^{2+}). The structures[4,5] of these complexes show a rhomb-like M_4O_{16} unit bridging two trivacant heteropolytungstate moieties $\{PW_9O_{34}\}$ and $\{P_2W_{15}O_{56}\}$ derived from the well-known Keggin and Dawson–Wells complexes, respectively (Figure 1). On the other hand, we have also extended this study to M = Mn^{2+} and Ni^{2+}. We have found that while in the manganese compounds of both Keggin and Dawson–Wells derivatives the structures of the anions are maintained, in the nickel compound of the Keggin derivative a novel type of anion formed by a triangular cluster of Ni^{2+} encapsulated by $\{PW_9O_{34}\}$ and $\{WO_6\}$ moieties is obtained.[6]

The rational syntheses of the Co, Cu, and Zn heteropolyanions, leading to isomerically pure products, were reported in 1987 by Finke, Droege, and Domaille.[7] These authors found that the Cu^{2+} product $[Cu_4(H_2O)_2(PW_9O_{34})_2]^{10-}$ is different from the Zn and Co derivatives and from $[Cu_4(H_2O)_2(P_2W_{15}O_{56})_2]^{16-}$ in that it is thermally unstable in solution. Thus, the thermolysis in solution of $[Cu_4(H_2O)_2(PW_9O_{34})_2]^{10-}$ gives rise to an unidentified product showing clear differences in both the X-ray diffraction powder pattern and the IR spectra when compared with the other members of the series and with $[Cu_4(H_2O)_2(PW_9O_{34})_2]^{10-}$. In fact, while the IR spectrum of $[Cu_4(H_2O)_2(PW_9O_{34})_2]^{10-}$ shows two bands in the P–O region (at 1015 and 1050 cm^{-1}) (Figure 2a), for the unidentified thermolysis product four bands are observed (at ca. 1040, 1070, 1100, and 1140 cm^{-1}).[7] Moreover, they found that the type of product obtained is largely dependent upon the experimental conditions (temperature and time); so, with the recrystallization conditions (100 °C, H_2O) used for the Co and Zn derivatives, the thermolysis product is obtained as the major product, while conducting the synthesis at lower temperature (<60 °C) and shorter times yields the desired copper complex $[Cu_4(H_2O)_2(PW_9O_{34})_2]^{10-}$.

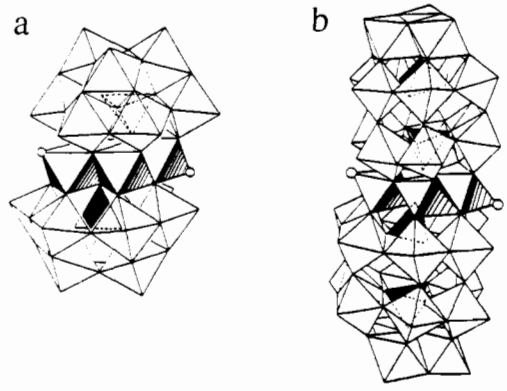

Figure 1. Structures of the $[M_4(H_2O)_2(PW_9O_{34})_2]^{10-}$ (Keggin derivative) (a) and $[M_4(H_2O)_2(P_2W_{15}O_{56})_2]^{16-}$ (Dawson–Wells derivative) (b) complexes. Each vertex of a polyhedron locates the center of an O atom, each white octahedron contains a W atom, each tetrahedron contains a P atom, and each shaded octahedron contains a M atom.

† Universidad de Valencia.
‡ CSIC.

(1) (a) Simmons, V. E. Doctoral Dissertation, Boston University, 1963; *Diss. Abstr.* **1963**, *24*, 1391. (b) Baker, L. C. W.; Baker, V. E. S.; Wasfi, S. H.; Candela, G. A.; Kahn, A. H. *J. Am. Chem. Soc.* **1972**, *94*, 5499. (c) Baker, L. C. W.; Baker, V. E. S.; Wasfi, S. H.; Candela, G. A.; Kahn, A. H. *J. Chem. Phys.* **1972**, *56*, 4917. (d) Kokoszka, G. F.; Padula, F.; Goldstein, A. S.; Venturini, E. L.; Azevedo, L.; Siedle, A. R. *Inorg. Chem.* **1988**, *27*, 59.

(2) (a) Casañ-Pastor, N. Doctoral Dissertation, Georgetown University, 1988. (b) Casañ-Pastor, N.; Baker, L. C. W. *J. Am. Chem. Soc.*, in press.

(3) (a) Gómez-Garcia, C. J.; Casañ-Pastor, N.; Coronado, E.; Baker, L. C. W.; Pourroy, G. *J. Appl. Phys.* **1990**, *67*, 5995. (b) Gómez-Garcia, C. J.; Coronado, E.; Borrás-Almenar, J. J. *Inorg. Chem.* **1992**, *31*, 1667. (c) Casañ-Pastor, N.; Bas-Serra, J.; Coronado, E.; Pourroy, G.; Baker, L. C. W. *J. Am. Chem. Soc.*, in press.

(4) (a) Weakley, T. J. R.; Evans, H. T.; Showell, J. S.; Tourné, G. F.; Tourné, C. M. *J. Chem. Soc., Chem. Commun.* **1973**, 139. (b) Evans, H. T.; Tourné, C. M.; Tourné, G. F.; Weakley, T. J. R. *J. Chem. Soc., Dalton Trans.* **1986**, 2699.

(5) Weakley, T. J. R.; Finke, R. G. *Inorg. Chem.* **1990**, *29*, 1235.

(6) (a) Gómez-Garcia, C. J. Doctoral Dissertation, Valencia University, 1991. (b) Gómez-Garcia, C. J.; Coronado, E.; Ouahab, L. *Angew. Chem., Int. Ed. Engl.* **1992**, *31*, 649.

(7) Finke, R. G.; Droege, M. W.; Domaille, P. J. *Inorg. Chem.* **1987**, *26*, 3886.

0020-1669/93/1332-0089$04.00/0

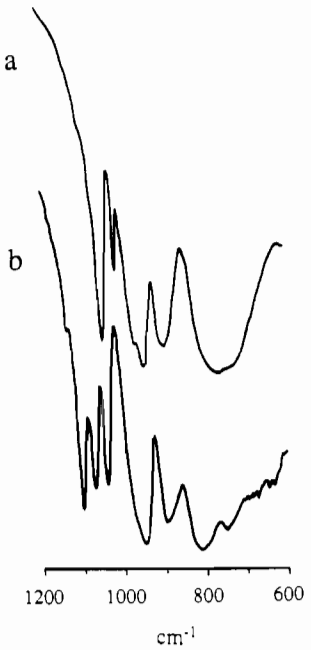

Figure 2. IR spectra of (a) $K_7Na_3[Cu_4(H_2O)_2(PW_9O_{34})_2]$ and (b) the related compound $K_{5.5}Na_{1.5}[PW_{10}Cu_2(H_2O)_2O_{38}]\cdot 13H_2O$.

On the other hand, we think that the thermolysis product obtained by heating a solution of the trimeric copper compound $[Cu_3(H_2O)_3(PW_9O_{34})_2]^{12-}$, as has been reported by Knoth et al.,[8] is likely the same unidentified product described by Finke.[7] Thus, although the potassium salt of the thermolysis product found by Knoth et al. analyzes for $K_{10}[Cu_4(H_2O)_2(PW_9O_{34})_2]$, the IR spectrum exhibits in the P–O region the four characteristic bands of the unidentified compound.

The phase reported in the present paper shows an IR spectrum (Figure 2b) which is very similar to that observed for the thermolysis product, raising the possibility that both complexes could be the same, or at least be closely related. Independently of such similarity, and in order to gain further understanding of the complex chemical behavior of a system containing $(PW_9O_{34})^{9-}$ and Cu^{2+} ions, this paper reports a structural and magnetic study of the product obtained from crystallization of the parent solution after standing a long period of time at room temperature. The combination of X-ray diffraction, magnetic susceptibility, and ESR studies allows us to identify the isomers present and the relative location of the pairs of Cu^{2+} ions in the structure.

Experimental Section

Preparation of $K_{5.5}Na_{1.5}[PW_{10}Cu_2(H_2O)_2O_{38}]\cdot 13H_2O$. Solid $CuCl_2\cdot 2H_2O$ (0.62 g, 3.6 mmol) was dissolved in 12 mL of distilled water. A 5.0-g sample of Δ-$Na_8HPW_9O_{34}\cdot 19H_2O$ (prepared according to the procedure of Finke et al.[7]) was added with stirring to this light blue solution. Once the Δ-$Na_8HPW_9O_{34}\cdot 19H_2O$ was dissolved, KCl (0.66 g, 1.8 mmol) was added to this light green solution, resulting in the immediate precipitation of a pale green solid. This solid was collected on a sintered-glass frit and redissolved in about 100 mL of hot water (60–70 °C). Any insoluble material was filtered out. The filtrate was kept covered, allowing very slow evaporation of the solvent, at room temperature. After several weeks shiny green crystals began to form. Two months later, the green cubic crystals were of adequate size for X-ray determination of the structure. The crystals were collected on a sintered-glass frit, washed carefully with cold water, and air dried under aspiration for several hours. The sample showed uniformity and apparent microscopic purity of all the crystals. From this sample the best crystals were chosen for X-ray structure determination, and the remaining were used for analysis and physical characterization. Analyses of this sample are consistent with the formula $K_{5.5}Na_{1.5}[PW_{10}Cu_2(H_2O)_2O_{38}]\cdot 13H_2O$. Anal. Calcd for $K_{5.5}Na_{1.5}[PW_{10}Cu_2(H_2O)_2O_{38}]\cdot 13H_2O$: K, 6.9; Na, 1.1; W, 58.9; Cu, 4.07; H_2O, 8.64. Found: K, 6.8, Na, 1.1; W, 59.6; Cu, 4.0; H_2O, 8.54.

Table I. Crystallographic Data for $K_{5.5}Na_{1.5}[PCu_2W_{10}O_{38}(H_2O)_2]\cdot 13H_2O$ (1)

formula $PCu_2W_{10}O_{48}H_{20}K_{5.5}Na_{1.5}$	T = 22 °C
fw 3034	λ = 0.709 26 Å
space group $Fm\bar{3}m$ (No. 225)	ρ_{calcd} = 4.15 g cm^{-3}
a = 21.329 (4) Å	μ = 256 cm^{-1}
V = 9703 (2) Å^3	$R(F_o)$ = 0.0459[a]
Z = 8	$R_w(F_o)$ = 0.0489[b]

[a] $R = \Sigma||F_o| - |F_c||/\Sigma|F_o|$. [b] $R_w = \Sigma w^{1/2}(|F_o| - |F_c|)/\Sigma w^{1/2}|F_o|$.

Crystallographic Study of $K_{5.5}Na_{1.5}[PW_{10}Cu_2(H_2O)_2O_{38}]\cdot 13H_2O$. Initially, precession photographs showed cubic symmetry (a = 10.66 Å) and no apparent systematic absences, consistent[9] with five possible space groups $P23$, $Pm3$, or $P\bar{4}3m$ (tetrahedral point symmetry) and $P432$ or $Pm3m$ (octahedral point symmetry). Nevertheless, very long exposure times (ca. 40 h, 15 mA, 35 kV) for interlayer reciprocal showed exceedingly weak spots consistent with an F-centered (pseudo-P) cubic cell (a = 21.329 (4) Å)[10].

A pale green crystal (stable open to air) was mounted on a CAD4 automatic diffractometer for data collection. Three standard reflections, measured every 100 reflections, showed no significant decay. Lattice parameters were obtained by the centering of 25 strong reflections at high angles ($2\theta \geq 25°$).

Lorentz and polarization corrections were applied to the intensity data. Later a semiempirical absorption correction[11] and extinction correction were also applied. Other important features of data collection and refinements are summarized in Table I.

The structure was solved by direct methods using MULTAN84[12] and developed with SHELX-76[13] using successive full-matrix least-squares refinements and difference Fourier syntheses. The superstructure spots observed on the precession photographs implied F centering and prompted us to refine the structure in space group $Fm3m$,[14] but the structure could be equally well refined, if not better, in space group $Pm3m$, with the superstructure spots being overlooked. In the latter case, we lose information concerning the disorder scheme of anions and cations, but the overall chemical information is still the same. Furthermore, the poor counting statistics of the weaker all-odd reflections seem to yield poorer reliability factors for the $Fm3m$ refinements.[15]

The final reliability factors for the F-centered structure were R = 0.0459 and R_w = 0.0489 ($w = 0.017/\sigma^2(F) + 0.0027F^2$) for 500 unique reflections with $I > 3\sigma(I)$ and 48 refined parameters. The four most intense peaks found in the final difference Fourier synthesis (3.8–2.8 e/Å^3) were less than 1 Å away from W. This is not surprising in view of the Cu substitution and the infeasibility of refining the positions of Cu and W separately. Otherwise, the difference Fourier map was featureless (continuum ca. 1.2 e/Å^3). Atomic parameters (x, y, z, U_{ij}'s) are given in Table II and the supplementary material. Bond lengths and angles are given in Tables III and IV.

Physical Measurements. Susceptibility measurements were performed in the temperature range 2–300 K using a VTS SQUID magnetometer (900 Series, SHE Corp.). The experimental susceptibility data were corrected for a temperature-independent paramagnetism of 1.5×10^{-3} emu·mol^{-1}. Such a value had to be subtracted from the experimental

(8) Knoth, W. H.; Domaille, P. J.; Harlow, R. L. *Inorg. Chem.* **1986**, *25*, 1577.

(9) Space Group Symmetry. *International Tables for Crystallography*; Hahn, T., Ed.; Reidel: Dordrecht, The Netherlands, 1983; Vol. A.

(10) R. G, Finke, W. J. Randall, and T. J. R. Weakley (personal communication) have obtained what appears to be the same hydrolysis product. Their single-crystal X-ray analysis [Rigaku AFC6R diffractometer, Mo radiation, space group $Fm3m$, a = 21.287 (3) Å, Z = 8, R = 0.049, R_w = 0.061, S = 1.73 for 285 independent reflections with $I \geq 3\sigma(I)$] gave the same structure as reported here, including the substitutional disorder in the Keggin anions. We thank Prof. Finke and a reviewer of this paper for their suggestion of the presence of this F centering.

(11) PSISCAN: North, A. C. T.; Phillips, D. C.; Mathews, F. S. A Semiempirical Method of Absorption Correction. *Acta Crystallogr.* **1968**, *A24*, 351–359.

(12) Main, P.; Germain, G.; Woolfson, MULTAN-11/84, A System of Computer Programs for the Automatic Solution of Crystal Structures from X-Ray Difraction Data. University of York, 1984.

(13) Sheldrick, G. M. SHELX-76: A Program for Crystal Structure Determination. Cambridge University, 1976.

(14) This same symmetry has been found in several other substituted heteropolyanions.

(15) Refinements in space group $Pm3m$ that we had conducted on a preliminary set of data with a = 10.6634 (6) Å yielded final R = 0.0296 and R_w = 0.0302.

Table II. Fractional Coordinates (×10⁴) and Equivalent Isotropic Temperature Factors for **1** (Estimated Standard Deviations in Parentheses)

atom	x/a	y/b	z/c	B_{eq},[a] Å²	occ
P	2500 (0)	2500 (0)	2500 (0)	0.93	0.04166
W	3675 (1)	3675 (1)	2456 (1)	1.42	0.4023
Cu	3675 (1)	3675 (1)	2456 (1)	1.42	0.0977
K1	0 (0)	2500 (0)	2500 (0)	2.93	0.125
K21	1825 (6)	0 (0)	0 (0)	3.29	0.0863 (19)
K22	3397 (27)	0 (0)	0 (0)	8.42	0.0387 (19)
Na	1075 (26)	0 (0)	0 (0)	4.52	0.0417
O1	2916 (4)	2916 (4)	2084 (4)	1.48	0.16666
O2	3907 (4)	3038 (3)	3038 (3)	1.82	0.5
O3	4091 (4)	3195 (3)	1805 (3)	1.46	0.5
O4	4257 (4)	4257 (4)	2590 (5)	2.98	0.5
OW	0 (0)	0 (0)	0 (0)	5.95	0.0208
OW1	0 (0)	1122 (7)	1122 (7)	3.76	0.25
OW2	5000 (0)	3904 (19)	3904 (19)	1.74	0.0625

[a] Anisotropically refined atoms are given in the form of the isotropic equivalent displacement parameter, defined as $B_{eq} = (4/3)[a^2B(1,1) + b^2B(2,2) + c^2B(3,3) + ab(\cos\gamma)B(1,2) + ac(\cos\beta)B(1,3) + bc(\cos\alpha)B(2,3)]$.

Table III. Selected Bond Lengths and Intermetallic Separations (Å) in **1** (Estimated Standard Deviations in Parentheses)

O1–W	2.423 (0.009)	O4–K21	2.772 (0.024)
O2–W	1.906 (0.002)	OW1–K21	2.824 (0.024)
O3–W	1.940 (0.004)	OW2–K22	2.576 (0.062)
O4–W	1.778 (0.012)	OW1–Na	2.394 (0.050)
O1–P	1.538 (0.015)	W···W	3.677 (0.001)
O2–K1	2.841 (0.018)	W···W	3.412 (0.001)
O3–K1	2.857 (0.018)	P···W	3.546 (0.001)

Table IV. Selected Bond Angles (deg) in **1** (Estimated Standard Deviations in Parentheses)

O1–P–O1	109.5 (0.0)	O3–W–O3	88.2 (0.5)
O2–W–O1	84.8 (0.3)	O4–W–O3	99.5 (0.3)
O3–W–O1	73.6 (0.3)	P–O1–W	125.6 (0.3)
O4–W–O1	170.1 (0.5)	W–O1–W	89.5 (0.4)
O2–W–O2	86.9 (0.5)	W–O2–W	149.5 (0.5)
O3–W–O2	88.4 (0.4)	W–O3–W	123.2 (0.4)
O4–W–O2	102.3 (0.4)		

susceptibility in order to obtain a constant value of the $\chi_m T$ product at high temperatures and account for the diamagnetism of the sample and the TIP contribution.[3] The magnetic susceptibility data were then fitted to the following equation, where the first two terms refer to the susceptibilities of two exchange-coupled Cu^{2+} ions and the third one refers to a Cu^{2+} paramagnetic contribution:[16]

$$\chi_m = (2Ng^2\beta^2kT)[A/(3 + e^{-2J_a/kT}) + B/(3 + e^{-2J_b/kT}) + (1 - A - B)/4] \quad (1)$$

In this expression N, β, and k have their usual meanings, g is the Landé factor of the Cu^{2+} ion, J_a and J_b are the exchange parameters of the two pairs (the exchange Hamiltonian is written as $H = -2JS_1S_2$), A and B are the corresponding molar fractions, and, finally, $(1 - A - B)$ is the molar fraction of noninteracting Cu^{2+} pairs.

Infrared spectra were obtained in KBr disks with a Perkin-Elmer 1750 FTIR spectrometer. EPR spectra were recorded at X-band on a Bruker ER 200D spectrometer equipped with a helium cryostat. Spectra at Q-band were recorded on a Varian spectrometer.

Results and Discussion

Structure. In the first stage of the structure determination it was found that the title compound consisted of a heteropolyanion with the known α-Keggin structure and K^+ counterions. The tetrahedral site in the anion is occupied by phosphorus, which occupies $\bar{4}3m$ sites at $^1/_4, ^1/_4, ^1/_4$ in the F cubic cell. Neighboring anions are rotated 90° about the $\bar{4}$ axis of the molecule (Figure 3), but this rotation leaves the overall metal network virtually unchanged, affecting mostly the oxygen atoms coordinated to phosphorus. This is why the F symmetry is only hardly recognizable in the diffraction pattern, which shows a clear pseudo-P symmetry.

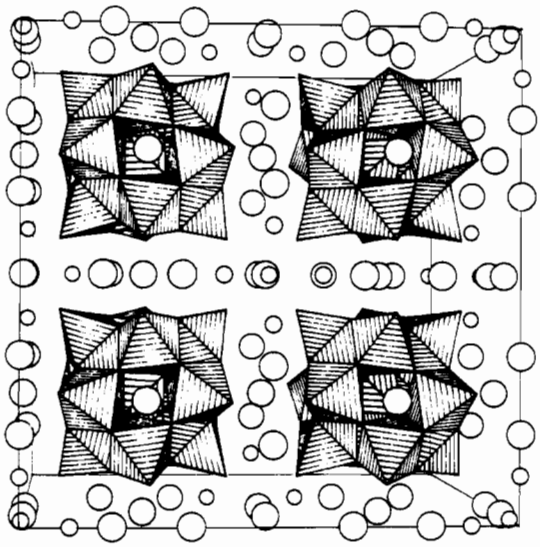

Figure 3. Packing diagram (STRUPLO[19]) of $K_{5.5}Na_{1.5}[PW_{10}Cu_2(H_2O)_2O_{38}]\cdot 13H_2O$ showing the alternating orientation of the anion and the disorder of the cations in the F unit cell (for clarity we show only the contents of the top half of the unit cell). Large circles are K^+ ions, small circles are Na^+ ions (partially occupied), W(Cu) atoms occupy the center of the octahedra, and phosphorus atoms are at $^1/_4, ^1/_4, ^1/_4$ in the unit cell. Water molecules are not shown for clarity.

Once the gross structural model had been established, it was necessary to determine the presence and location of counterions in the structure as well as the substitution of Cu for W ions.

We found an ordered K^+ ion with full occupancy (K1, three K^+ ions/anion, bisphenoidal coordination), a second K^+ ion disordered between two positions (K21, K22, in total three K^+ ions/anion, both in a square antiprism), and a sodium ion partially occupying a 12-coordinated site (one Na^+ ion/anion).

Concerning the substitution of Cu for W, it was evident that the only chemically reasonable site for Cu was in the place of W in the anion (the possibility of Cu occupying the tetrahedral site was unreasonable, given the short bond lengths with O1, typical of P–O bonds[17]). Cu coordinates and thermal parameters were thus fixed equal to those of W. A final refinement fixing the total occupancy at the metal site to the expected value Occ(W) + Occ(Cu) = 0.5 but freeing the Cu/W ratio led to a molar ratio of 0.24 (i.e. 2.3 Cu/9.7 W), very close to the 2 Cu/10 W expected for a disubstituted Keggin anion of the type $PW_{10}Cu_2O_{40}$. This refined ratio should be taken cautiously, given its correlation with the scale factor, but its good agreement with the chemical analyses seems to confirm the correctness of the structural model refined.

According to all the above, we formulate the anion as $[PW_{10}Cu_2(H_2O)_2O_{38}]^{7-}$ where the coordinated water molecules would be most likely associated to the Cu ions.[17] The X-ray refinement shows only eight crystallization water molecules. The rest (up to 13) must correspond to water molecules heavily disordered in the lattice that cannot be properly located nor refined. Chemical analyses showed the presence of ca. 5.5 K^+ ions and ca. 1.5 Na^+ ions per anion and guided us in setting the cationic

(16) Carlin, R. L. *Magnetochemistry*; Springer-Verlag: Berlin, Heidelberg, 1986.

(17) (a) Baker, L. C. W.; Figgis, J. S. *J. Am. Chem. Soc.* **1970**, *92*, 3794. (b) Figgis, J. S. Doctoral Dissertation, Georgetown University, 1970. (c) Spirlet, M. R.; Busing, W. R. *Acta Crystallogr.* **1978**, *B34*, 907. (d) Brown, G. M.; Noe-Spirlet, M. R.; Busing, W. R.; Levy, H. A. *Acta Crystallogr.* **1977**, *B33*, 1038. (e) Evans, H. T., Jr.; Pope, M. T. *Inorg. Chem.* **1984**, *23*, 501.

(18) Pope, M. T. *Heteropoly and Isopoly Oxometalates*; Springer-Verlag: Berlin, 1983.

(19) Fisher, R. X. *J. Appl. Crystallogr.* **1985**, *18*, 258.

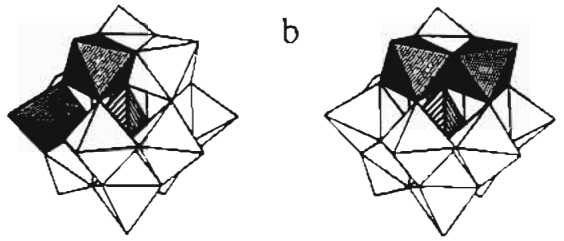

Figure 4. STRUPLO[19] drawings of the heteropolyanion showing the two possible isomers containing neighboring Cu ions: (a) connected through a corner oxygen atom (O2); (b) connected through an edge of their coordination octahedra (O1 and O3).

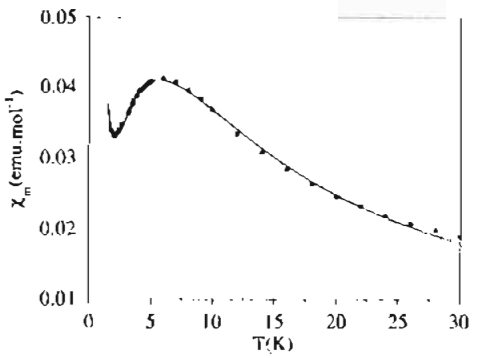

Figure 5. Plot of χ_m versus T for $K_{5.5}Na_{1.5}[PW_{10}Cu_2(H_2O)_2O_{38}]\cdot 13H_2O$. The solid line represents the best fit of eq 1.

contents of our structural model. Nevertheless, the evident disorder of all the cations (except K1) made it difficult to unambiguously find the position and amount of each ion. We refined each type of cation in the most likely sites (i.e. Na with the shorter bonds), but some degree of mutual disorder cannot be ruled out. On the other hand, the final model yields reasonable temperature factors for all of them, and the partial occupation factors refined make compatible the coexistence in the lattice of Na and K21 (1.6 Å apart on the average).

The disorder of W–Cu ions in the anion, as deduced from the diffraction data, does not imply any particular distribution of the two Cu ions in the molecule. If we consider the cases where the two are in neighboring sites, there will be two isomers present in the structure: a substituted Keggin anion of the type $PW_{10}Cu_2$ with two CuO_6 octahedra sharing a corner (Figure 4a) and the analogue with the two CuO_6's sharing an edge (Figure 4b). These two isomers are magnetically inequivalent; the former has a single bridge with a bridging W–O–W angle of 148°, while the latter has a double bridge and a W–O–W angle of 125.5°. However, the presence of complexes with nonconnected Cu ions cannot be ruled out on the basis of the diffraction data.

Magnetic Properties. The title compound shows a rounded maximum of susceptibility centered at $T \approx 6$ K (see Figure 5), consistent with the presence of antiferromagnetically coupled copper pairs in the heteropoly complex. On the other hand, the small increase of the susceptibility for $T < 2$ K indicates the presence of only a few percent of magnetically isolated Cu^{2+} ions. This last probability accounts for the presence of $PW_{10}Cu_2$ complexes in which the two Cu^{2+} ions are not adjacent, although the possibility of some $PW_{11}Cu$ impurity cannot be excluded.

Given the possible presence in the structure of two magnetically inequivalent isomers when the two copper ions are on adjacent sites (see Figure 4), the experimental data have been fitted by means of a model that considers two independent $S = {}^1/_2$ pairs with different exchange-coupling constants, namely J_a and J_b, and a paramagnetic $S = {}^1/_2$ contribution that accounts for the presence of magnetically isolated Cu ions (expression 1). Notice that, as expression 1 is written, the amount of paramagnetic contribution refers to the amount of heteropoly complexes containing nonadjacent CuO_6 octahedra. The molar fractions of these moieties have been allowed to vary in the fitting procedure (see Experimental Section). A very satisfactory fit of the experimental data (full line in Figure 5) has been obtained from the set of parameters reported in Table V. It must be noted that, despite the larger number of adjustable parameters, reliable values of the two exchange couplings and of the amount of complexes containing magnetically isolated Cu ions result from the fitting procedure. Conversely, the molar fractions of the two pairs are strongly correlated, so that only approximate values of these two parameters can be extracted.

Table V. Best Fit Parameters of $K_{5.5}Na_{1.5}[PW_{10}Cu_2(H_2O)_2O_{38}]\cdot 13H_2O$ from Magnetic Susceptibility Data

	g	J, cm^{-1}	amt, %
pair a	2.2	−7.6	39.0
pair b	2.2	−3.2	52.5
isolated Cu^{2+}	2.2	–	8.5[a]

[a] This amount corresponds to the amount of Keggin complexes containing nonadjacent CuO_6 octahedra.

In view of the larger Cu–O–Cu bridging angle shown by the isomer in which the two CuO_6's are sharing a corner (148° compared to 125.5°), we can associate the strongest antiferromagnetic exchange coupling, $J_a = -7.6$ cm^{-1}, with this isomer and the weaker one, $J_b = -3.2$ cm^{-1}, with the isomer in which the two CuO_6's are sharing an edge. In the former case, the two metal orbitals containing the unpaired electron (of the type $d_{x^2-y^2}$) are pointing toward the single oxo bridge. In the second case, a very similar situation occurs, since the distortions of the octahedra, with the water molecules determining the axial directions, are such that the $d_{x^2-y^2}$ metal orbitals are directed toward a common oxo bridge. For corner-sharing situations a stronger antiferromagnetic interaction is expected as the bridging angle approaches 180°, since the magnetic orbitals are then more favorably positioned to overlap,[20] thus justifying the above assignment. Further support for this assignment may be obtained by comparing these values with those calculated for the related heteropoly complex $[Cu_4(H_2O)_2(PW_9O_{34})_2]^{10-}$ (see Figure 1). In fact, in this complex the exchange between two adjacent copper sites sharing an edge has been found[3b] to be −3.5 cm^{-1}, a value very close to the smaller of the two J values reported here, which we assign to pair b.

The above discussion has shown that (1) in each heteropoly complex the Cu ions are preferentially occupying neighboring sites and (2) the two possible isomers, with two CuO_6 octahedra sharing a corner (a) or an edge (b), are present in similar amounts.

EPR Spectra. The thermal variation of the polycrystalline powder EPR spectra at X-frequency is shown in Figure 6. Its interpretation is not straightforward, but it becomes clearer in view of the magnetic susceptibility results. At 4.2 K the central part of the spectrum shows a typical axial spectrum with $g_\parallel = 2.36$, $g_\perp = 2.06$, and a four-line hyperfine structure on the parallel component, which is in agreement with the presence of isolated Cu^{2+} ions. Besides these signals, a typical spectrum of a spin triplet,[21] with signals at ca. 2300, 2800, 3500, and 3900 G and a half-field signal at ca. 1600 G, is observed. According to the exchange parameters (see Table V), only the triplet state of pair b is expected to be significantly populated at 4.2 K (the ratio between the thermal populations of the two triplets is pair a/pair b ≈ 1/20). Then, these triplet features are to be associated with pair b. A good fit of the positions of the signals has been obtained from the following assignments: $H(z1) \approx 2300$ G, $H(z2) \approx 3900$ G, $H(x1) \approx 2800$ G, $H(y1) \approx 3000$ G, and $H(y2) \approx H(x2) \approx 3500$ G (see Figure 7a). This simulation allows us to obtain the

(20) Hay, P. J.; Thibeault, J. C.; Hoffmann, R. *J. Am. Chem. Soc.* **1975**, *97*, 4884.
(21) Wasserman, E.; Snyder, L. C.; Yager, W. A. *J. Chem. Phys.* **1964**, *41*, 1763.

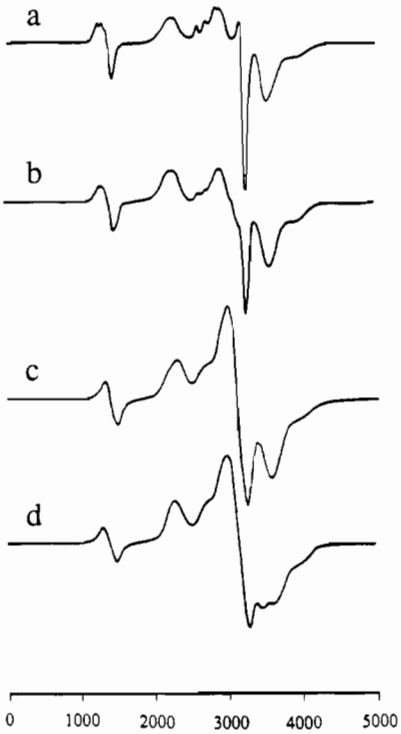

Figure 6. Thermal variation of the EPR spectra of $K_6Na[PW_{10}Cu_2(H_2O)_2O_{38}]\cdot 13H_2O$ at X-frequency: (a) T = 4.2 K; (b) T = 12 K; (c) T = 60 K; (d) T = 300 K.

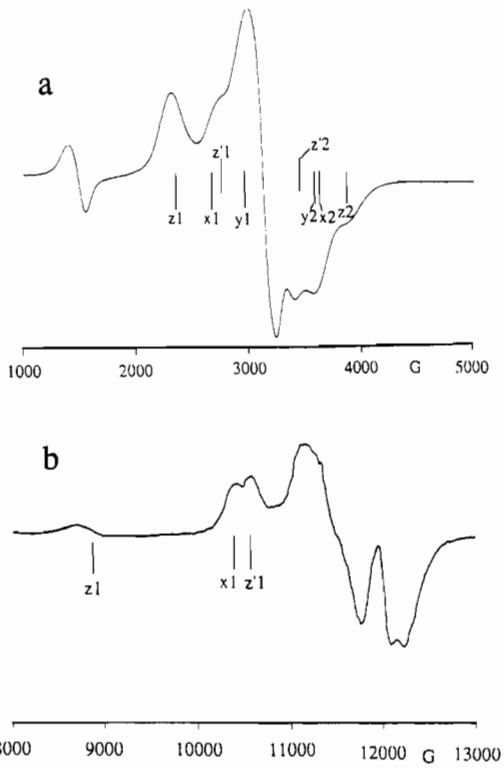

Figure 7. (a) Polycrystalline powder EPR spectra of $K_6Na[PW_{10}Cu_2(H_2O)_2O_{38}]\cdot 13H_2O$ at room temperature showing the position of the bands obtained with the simulation, where x, y, and z stand for dimer a and x', y', and z' stand for dimer b (see text). (b) Q-Frequency spectrum of the same sample under the same conditions showing the splitting of the shoulder centered at ca. 2800 G at X-frequency.

following values of the zero-field splitting and Landé parameters for the triplet of pair b: $|D_b| = 0.076 \pm 0.002$ cm^{-1}, $|E_b| \approx 0.005 \pm 0.002$, $g_{bx} = 2.06$, $g_{by} = 2.01$, and $g_{bz} = 2.12$.

As the temperature increases, we observe an increase in intensity and width of the line centered at 3100 G at the expense of the paramagnetic signal, which becomes nearly masked at room temperature, together with the appearance of a new feature at ca. 3400 G. These changes may arise from the thermal population of the triplet of pair a, lying 15.2 cm^{-1} above the singlet ground state. Since these changes seem to be limited in the region 2700–3400 G, a very small value of the axial zero-field splitting of triplet of pair a is predicted. Thus, taking $H(z'2) \approx 3400$ G and $g_{az} \approx g_{bz} = 2.12$, a value of $|D_a| \approx 0.03$ cm^{-1} may be estimated. In such a case, the signal z'1 is expected to be located around 2800 G, very close to $H(x1)$ of pair b. Such an assumption has been confirmed by the Q-band room-temperature spectrum (Figure 7b), which shows that the feature observed at ca. 2800 G in the X-band as a shoulder can in fact be resolved into two signals centered at 10 400 and 10 600 G (i.e., 2750 and 2800 G in X-band).

Bearing in mind that the anisotropic part of the exchange may have a magnitude of order $|D| = (\Delta g/g)^2|J|$, where Δg describes the orbital contribution to the **g** tensor,[22] the larger D value would correspond to that pair with a larger J value (a). However, in our case, we observe the opposite trend. This is probably due to the dipolar contribution to D, which is larger for the pair with a smaller J value (b), since its intermetallic distance is smaller (3.1 Å compared to 3.5 Å). Then, in view of the weakness of the resulting exchange-coupling constants, the dipolar contribution may be stronger in this case than the exchange contribution.

Finally, in order to check the reproducibility of the preparation, we examined the EPR spectra of a second preparation. We noticed that these spectra were, within experimental error, identical to those reported in Figures 6 and 7, indicating that the relative amounts of the isomers and monomer did not change significantly from one sample preparation to the next.

IR Spectra. As noted above (see Figure 2), the IR spectrum of the salt of the anion $[Cu_4(H_2O)_2(PW_9O_{34})_2]^{10-}$ in the P–O region shows clear differences from that of the title compound. Thus, while the IR spectrum of the former shows two bands in the P–O region, for the latter as many as four bands are observed in this region. Such a difference may be now understood on the basis of the structural features of these compounds, which determine different distortions in the PO_4 tetrahedron. In the former there is only one type of distortion (the Cu^{2+} ions are bonded to only one oxygen of the PO_4 tetrahedron). For a distorted PO_4 tetrahedron, a maximum of three bands is expected.[8] The larger number of bands in the spectrum of the title compound is in agreement with the presence of two types of distortions of the PO_4 groups as a consequence of the presence of two different isomers: in the isomer where the two CuO_6 octahedra share a corner, two O atoms bonded to P are bonded to the Cu atoms, while in the case where the CuO_6 octahedra are sharing an edge only one O bonded to P bridges the two Cu atoms.

Acknowledgment. This work was supported by The Comisión Interministerial de Ciencia y Tecnologia (Grant MAT89-177), by the Intitució Valenciana d'Estudis i Investigació, and by a Spanish-French Integrated Action grant. We are deeply grateful to the Centre de Recherches Paul Pascal (Talence, France) for the use of the SQUID magnetometer and to C. Zanchini from the Department of Chemistry of the University of Florence for her help with the low-temperature EPR measurements. N.C.-P. and P.G.-R. thank the Ministerio de Educación y Ciencia for a grant (CE89-0010-C02-02), and C.J.G.-G. thanks the Ministerio de Educación y Ciencia for a fellowship.

Supplementary Material Available: A table of thermal parameters (U's) and estimated standard deviations (1 page). Ordering information is given on any current masthead page.

(22) Bencini, A.; Gatteschi, D. *EPR of Exchange Coupled Systems*; Springer Verlag: Berlin, 1990.